Effect of Postnatal Development on Calcium Currents and Slow Charge Movement in Mammalian Skeletal Muscle

KURT G. BEAM and C. MICHAEL KNUDSON

From the Department of Physiology and Biophysics, University of Iowa School of Medicine, Iowa City, Iowa 52242, and the Department of Physiology, Colorado State University, Fort Collins, Colorado 80523

ABSTRACT   Single- (whole-cell patch) and two-electrode voltage-clamp techniques were used to measure transient (I_{fast}) and sustained (I_{slow}) calcium currents, linear capacitance, and slow, voltage-dependent charge movements in freshly dissociated fibers of the flexor digitorum brevis (FDB) muscle of rats of various postnatal ages. Peak I_{fast} was largest in FDB fibers of neonatal (1–5 d) rats, having a magnitude in 10 mM external Ca of 1.4 ± 0.9 pA/pF (mean $\pm$ SD; current normalized by linear fiber capacitance). Peak I_{fast} was smaller in FDB fibers of older animals, and by ~ 3 wk postnatal, it was so small as to be unmeasurable. By contrast, the magnitudes of I_{slow} and charge movement increased substantially during postnatal development. Peak I_{slow} was 3.6 ± 2.5 pA/pF in FDB fibers of 1–5-d rats and increased to 16.4 ± 6.5 pA/pF in 45–50-d-old rats; for these same two age groups, Q_{max}, the total mobile charge measurable as charge movement, was 6.0 ± 1.7 and 23.8 ± 4.0 nC/μF, respectively. As both I_{slow} and charge movement are thought to arise in the transverse-tubular system, linear capacitance normalized by the area of fiber surface was determined as an indirect measure of the membrane area of the t-system relative to that of the fiber surface. This parameter increased from 1.5 ± 0.2 μF/cm^2 in 2-d fibers to 2.9 ± 0.4 μF/cm^2 in 44-d fibers. The increases in peak I_{slow}, Q_{max}, and normalized linear capacitance all had similar time courses. Although the function of I_{slow} is unknown, the substantial postnatal increase in its magnitude suggests that it plays an important role in the physiology of skeletal muscle.

INTRODUCTION

An action potential causes a skeletal muscle fiber to contract, a process known as excitation-contraction (E-C) coupling. Two important structural elements for E-C coupling are infoldings of the surface membrane, termed transverse-tubules (t-tubules or t-system), and a wholly internal membranous compartment termed the sarcoplasmic reticulum (SR). During E-C coupling, depolarization of the t-system causes the SR to release calcium, which in turn causes contraction (Costantin, 1975; Endo, 1977). The events that link t-system depolarization to SR calcium release

remain to be established. One event likely to be involved is measurable as an electrical signal termed charge movement. Charge movement, which has been measured in both amphibian (Schneider and Chandler, 1973; Chandler et al., 1976; Adrian and Almers, 1976) and mammalian (Hollingworth and Marshall, 1981; Dulhunty and Gage, 1983; Simon and Beam, 1983, 1985a; Lamb, 1986a) skeletal muscle, has been hypothesized to represent the voltage-induced change in the configuration of a "sensor" molecule embedded in the t-system membrane; this reconfiguration in turn is hypothesized to cause SR calcium release (Schneider and Chandler, 1973).

An alternative hypothesis for E-C coupling is that a small amount of calcium entering the fiber from the extracellular space triggers a large release of calcium ions from the SR (Endo et al., 1970; Ford and Podolsky, 1970). Consistent with this hypothesis, a slowly activated calcium current (I_{slow}) has been measured in both amphibian (Beaty and Stefani, 1976; Stanfield, 1977; Sanchez and Stefani, 1978; Almers and Palade, 1981) and mammalian (Potreau and Raymond, 1980; Donaldson and Beam, 1983; Walsh et al., 1986) skeletal muscle fibers. However, the slow time course of this current compared with the action potential makes it seem unlikely that it is involved in E-C coupling (Sanchez and Stefani, 1978). Moreover, blocking the current pharmacologically does not abolish E-C coupling in adult frog muscle (Gonzalez-Serratos et al., 1982). Thus, the function of I_{slow} is not known.

A possibility is that I_{slow} is vestigial in adult muscle and important only to the function of developing muscle. Specifically, one might imagine that I_{slow} is important for E-C coupling in developing muscle. E-C coupling might well be different since the diameter of neonatal mammalian skeletal muscle fibers is only about one-fifth that of adult fibers (Luff and Atwood, 1971), and neonatal fibers have very little t-system (Schiaffino and Margreth, 1969; Luff and Atwood, 1971). Calcium entering into small-diameter fibers with a sparse t-system might well have a function that is no longer important in the much larger adult fibers with their extensive t-system. With this hypothesis in mind, we examined calcium currents and charge movement in acutely dissociated fibers of the flexor digitorum brevis muscle of rats of various ages.

We have found two calcium currents in neonatal muscle, I_{fast} and I_{slow}. I_{fast} disappears after the first few weeks postnatal. By contrast, both I_{slow} and charge movement are present both neonatally and later in development. In fact, the magnitude of both increases more than fivefold during postnatal development. The postnatal increase in the magnitude of I_{slow} is the opposite of what one might expect for a vestigial current, and suggests instead that I_{slow} reflects a functionally important component of adult muscle.

A preliminary account of some of these results has appeared (Knudson et al., 1986).

METHODS

All experiments were carried out with fibers enzymatically dissociated (Beam and Knudson, 1988) from the flexor digitorum brevis (FDB), a fast-twitch (Carlsen et al., 1985) muscle of the rat. Currents were measured using the whole-cell configuration of the patch-clamp technique or, for the larger fibers from older animals, a two-electrode voltage clamp. For both the whole-cell patch clamp and the two-electrode clamp, pipettes were pulled from borosilicate

glass and filled with a solution that contained (millimolar): 140 Cs-aspartate, 5 Mg-aspartate$_2$ or 5 MgCl$_2$, 10 Cs$_2$EGTA, 10 HEPES, pH 7.4 with CsOH. Pipette resistances ranged from 1.5 to 2.5 MΩ. The whole-cell patch clamp was implemented as described by Hamill et al. (1981; additional details are given in Beam and Knudson, 1988). For the two-electrode clamp, one pipette was used to measure potential and the other was used to pass current. The output of the current-passing pipette was controlled via a conventional, high-voltage-output, two-electrode voltage-clamp circuit. Each of the two pipettes was brought up to the surface of the fiber and gentle suction was applied until a high-resistance (>100 MΩ) seal was established; strong suction was then used to rupture the patch of membrane beneath the pipette. To monitor seal formation and patch rupture, the potential at the top of the pipette was measured in response to a square wave applied to the pipette via a 1-GΩ resistor. To decrease their capacitance, both pipettes were coated with Q-dope (G.C. Electronics, Rockford, IL). Separate agar-bridge electrodes were used for sensing the bath potential and for providing the bath ground for current flow. The bath solutions used were (millimolar): "50 Ca": 50 Ca^{++}, 85 TEA$^+$, 185 Cl$^-$; "10 Ca": 10 Ca^{++}, 145 TEA$^+$, 165 Cl$^-$ (or 20 Cl$^-$ and 145 Br$^-$). Both solutions were buffered with 10 HEPES, titrated to pH 7.4 with CsOH.

Nonlinear capacitative currents were measured with fibers bathed in 10 Ca solution; usually 10 μM TTX was also present, and in some cases 1 mM Cd was present as well. For measurements made with the whole-cell patch clamp, the feedback resistor in the headstage was 10 MΩ. For measurements made with the two-electrode clamp, the clamp current was determined as the voltage drop across a 1-MΩ resistor in series with the current-passing pipette. For both voltage-clamp methods, linear components of capacitative and leak currents were canceled as completely as possible with a three-time-constant analog leak-subtractor before additional gain was taken on the signal from the current-measuring amplifier. Remaining linear components of current were removed from test currents by digital scaling and subtraction of a control current elicited by a 20–30-mV depolarization or hyperpolarization from the holding potential (the same control current was used to calculate the linear fiber capacitance). Because the measured charge movements were similar for the depolarizing and hyperpolarizing control pulses, we concluded that little charge moves at membrane potentials less than or equal to −50 mV. To help prevent saturation or slew-rate limiting of amplifiers, voltage-clamp command pulses were exponentially rounded with a time constant of 50–300 μs. After subtraction of a sloping baseline as necessary (Horowicz and Schneider, 1981), Q_{ON} and Q_{OFF} were calculated by integrating the ON and OFF charge movement transients.

The dependence of Q_{ON} and Q_{OFF} on test potential (V) was quantified by fitting the data according to a two-state Boltzmann model for the distribution of charge:

$$Q = Q_{max}/\{1 + \exp[-(V - \overline{V})/k]\}, \qquad (1)$$

where Q_{max} represents the maximum charge that can be moved, $\overline{V}$ is the potential at which half the charge has moved, and k is a slope factor. The parameters Q_{max}, $\overline{V}$, and k were initially adjusted manually to give a visual best fit of the data. The computer was then used to calculate the sum of the squared deviations between the calculated curve and the data points as each of these three parameters was stepped through a range of values: ±8 mV in 1-mV steps for $\overline{V}$ and ±40% in 5% steps for Q_{max} and k. The combination of parameters that minimized the sum of the squared deviations was taken as the best fit.

The two-state Boltzmann expression was also used to quantify activation of the slow calcium current. Specifically, plots of conductance vs. voltage were fitted according to the expression

$$g(V) = g_{max}/\{1 + \exp[-(V - \overline{V})/k]\}, \qquad (2)$$

where $g(V)$ is the slow calcium conductance at test potential V, g_{max} represents the maximum conductance activated by strong test potentials, $\overline{V}$ is the midpoint of the activation curve (i.e.,

the potential for activation of half-maximal conductance), and k has the same meaning as in Eq. 1. The parameters g_{max}, $\bar{V}$, and k were adjusted to minimize the sum of the squared deviations between the data points and the curve calculated with Eq. 2. The conductance $g(V)$ was calculated from the measured slow calcium current with the expression

$$g(V) = I_{slow}/(V - V_{rev}),$$

where I_{slow} represents the peak inward slow calcium current measured at test potential V, and V_{rev} was determined by linear extrapolation of the falling limb of the peak I-V curve. (In cells with a large I_{fast}, care was taken to calculate peak I_{slow} at a time when the decay of I_{fast} was essentially complete.)

RESULTS

Postnatal Changes in Calcium Currents

Fig. 1 compares calcium currents recorded from FDB muscle fibers of a 2-d-old (A) and a 19-d-old (B) rat. In the fiber from the 2-d rat, two distinct calcium currents are present, a transient current (I_{fast}) selectively activated by test potentials from −40 to −10 mV, and an additional, maintained current (I_{slow}) activated by test depolarizations ≥0 mV. The presence of these two calcium currents in primary cultures of embryonic rat and mouse muscle, and in FDB muscle fibers of neonatal rats, has been previously documented (Beam et al., 1986; Cognard et al., 1986a; Beam and Knudson, 1988). For the fiber in Fig. 1 A, the amplitudes of I_{fast} and I_{slow} were comparable. This was typical of muscle fibers from animals 1 or 2 d old. The calcium currents recorded from the fiber of the 19-d-old rat (Fig. 1 B) are different in two major respects from those of the 2-d rat fiber. First, the test potentials from −40 to −10 mV, which elicited I_{fast} in the 2-d fiber, failed to elicit any appreciable time-dependent current in the 19-d fiber. Second, the I_{slow} current that is evoked by test pulses to ≥0 mV is >15-fold larger than I_{slow} in the 2-d fiber. Although fiber size increases between 2 and 19 d (~1.4-fold in diameter and 2.5-fold in length), the increase in the fiber surface area is much smaller than the increase in the magnitude of I_{slow}. The growth of a membrane system (i.e., the t-system) where slow calcium channels reside may be involved in the increase of I_{slow} (see below).

To get a more complete picture of the effect of postnatal development on I_{fast} and I_{slow}, calcium currents were measured in fibers acutely dissociated from FDB muscles of various-aged rats. For each fiber, the value at the peak of the largest I_{fast} and of the largest I_{slow} were recorded. These values were normalized by the linear capacitance of the fiber, since the capacitance provides an indirect measure of the fiber's membrane area (see below). Fig. 2 illustrates data collected from rats aged 0–50 d. Peak I_{fast} is large at birth and then undergoes a gradual decline and disappears entirely by 3–4 wk postnatal. By contrast, peak I_{slow} is relatively small at birth but increases about fivefold during the first 4 wk postnatal, after which it remains at relatively constant level. The postnatal developmental increase in the magnitude of peak I_{slow} suggests that the slow calcium channel protein plays an important role in skeletal muscle function.

Postnatal Changes in Charge Movement

As described in the Introduction, a nonlinear capacitative current, or "charge movement," which is thought to be involved in E-C coupling, has been found to be present in adult skeletal muscle of several different species. Fig. 3, A and C, illustrates similar
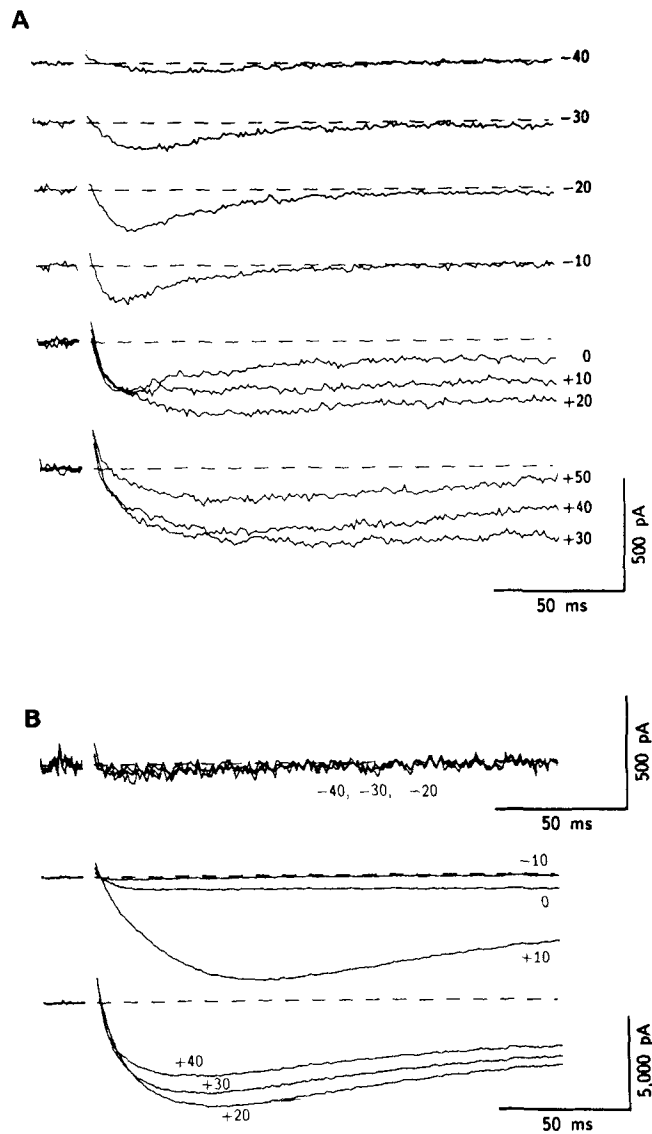
A

B

FIGURE 1. Developmental change in muscle calcium currents. Calcium currents are illustrated for FDB muscle fibers from a 2-d (*A*) and a 19-d (*B*) rat. (*A*) Fiber A76; four points blanked; 10 Ca bath solution; holding potential (HP) = -90, C = 175 pF. (*B*) Fiber D48, three points blanked; 10 Ca solution + 10 μM TTX; HP = -80; C = 430 pF.

nonlinear capacitative currents measured in neonatal rat muscle fibers. These were measured in response to 10-ms depolarizations from the holding potential to the test potential indicated to the right of each trace. By integrating the ON transient that follows the onset of the test pulse, one obtains Q_{ON}, the amount of charge that moves upon depolarization. Similarly, Q_{OFF}, the charge that moves upon repolarization, is the integral of the OFF transient that follows the cessation of the test pulse. Plots of

Q_{ON} and Q_{OFF} vs. test potential are illustrated in Fig. 3, B and D. As in adult skeletal muscle, the absolute magnitudes of Q_{ON} and Q_{OFF} are nearly equal. Also, both Q_{ON} and Q_{OFF} initially increase in size as the test pulse is made larger and then saturate for sufficiently large depolarizations.

The charge movements in Fig. 3 A were measured in an FDB fiber of a 5-d rat, while the charge movements in Fig. 3 C were measured in an FDB fiber of a 21-d rat. The charge movements from the two different-aged rats have similar properties, with the exception that Q_{max}, the maximum amount of charge that moves for a strong
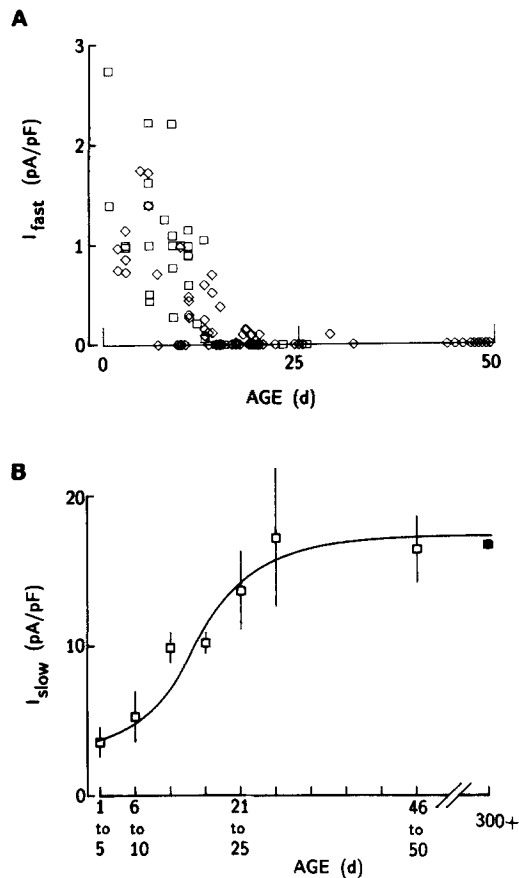

FIGURE 2. Peak I_{fast} and peak I_{slow} as a function of postnatal age. (A) I_{fast} was measured in either 50 mM Ca (squares) or 10 mM Ca (diamonds). For each fiber, the magnitude of the largest peak I_{fast} was determined and normalized by the linear capacitance of that fiber. Three data points for 1-d FDB fibers in 50 mM Ca are not shown because they were offscale. For these three fibers, the peak I_{fast} was 11.3 ± 7.0 pA/pF. (B) Normalized peak I_{slow} as a function of postnatal age. Each data point represents the average value obtained for fibers spanning a 5-d range of age. The error bars indicate ± SEM. The filled square is based on an average peak I_{slow} of 139 $\mu A/cm^2$ (Donaldson and Beam, 1983) and an average linear capacitance of 8.3 $\mu F/cm^2$ (T = ~20°C, Table II, Beam and Donaldson, 1983) measured with the three-microelectrode technique in omo-hyoid muscle fibers of adult (>300 d) rats. The smooth curve was arbitrarily drawn by eye through the data points.

depolarization, is ~20 times larger in the older rat. After normalization by linear fiber capacitance, Q_{max} in the older animal is still more than three times larger. However, as discussed later, this may not represent an increase in Q_{max} with respect to the membrane area of the t-system. The postnatal developmental increase in the normalized Q_{max} is illustrated in more detail in Fig. 4. As for peak I_{slow}, Q_{max} increased about fivefold during the first 4 wk postnatal, after which it remained at a fairly constant level. To permit a more direct comparison of the postnatal development of Q_{max} and peak I_{slow}, the same smooth curve that was shown superimposed on peak I_{slow} (Fig. 2 B) is also shown superimposed on the Q_{max} data.

Although the increase in Q_{max} represented the major postnatal change in muscle charge movements, there was also a small change in the charge movements' steady state voltage dependence. To characterize this voltage dependence, a least-squares procedure was used to fit Eq. 1 to plots of Q_{ON} and Q_{OFF} vs. test potential. This procedure yields values for $\bar{V}$, the midpoint of the charge-voltage relationship, and k, a parameter that determines the steepness of this relationship. The values for $\bar{V}$ were shifted positively in older rats. Specifically, the values (mean ± SD) of $\bar{V}$ were -9.3 ± 7.9 ($N = 6$), -0.6 ± 7.9 (9), and 2.6 ± 4.2 mV (5) for <15-, 15–25-, and >25-d FDB fibers, respectively. For the same three age groups, the values for k showed little difference, being 11.2 ± 4.9, 11.1 ± 3.5, and 11.5 ± 2.6 mV.

The midpoint of the activation curve for I_{slow} also appeared to shift positively with postnatal development. Thus, fits of the Boltzmann expression to conductance vs. voltage plots (see Methods) yielded values for $\bar{V}$ of 10.3 ± 7.5 (24), 12.4 ± 6.3 (30), and 16.1 ± 4.8 mV (15), respectively, for <15-, 15–25-, and >25-d FDB fibers; the values of k for these three age groups were 5.8 ± 1.7, 4.9 ± 1.4, and 7.1 ± 2.5 mV, respectively.

Postnatal Development of the T-System

As detailed in the Discussion, both the slow calcium current and charge movement are thought to arise within the t-system. Morphometric measurements of mouse skeletal muscle have revealed that the percentage of fiber volume occupied by the t-system increases about fivefold during the first few weeks postnatal (Luff and Atwood, 1971). This increase implies a concomitant increase in the membrane area of the t-system relative to that of the fiber surface. Thus, the developmental increases in Q_{max} and peak I_{slow} may be related to the developmental increase in relative t-tubular area. As an indirect measure of the latter, we determined the linear capacitance (C) and the fiber surface area (A_s) in individual fibers from rats of various ages. A_s was calculated, under the assumption of right-cylindrical geometry, from visual measurements of fiber length and diameter. Fig. 5 illustrates that C/A_s increases as a function of age. This increase implies that with postnatal development, membrane infolding is increasing the total membrane area compared with that calculated from fiber dimensions. In skeletal muscle, the t-tubular system accounts for a large component of membrane infolding. Thus, the data of Fig. 5 suggest that there is a postnatal increase in relative t-tubular area. The time course of this increase is strikingly similar to that of the postnatal increases in Q_{max} and I_{slow}, as can be seen by comparison of the data points with the smooth curve (the same one as in Figs. 2 B and 4). That all three increase postnatally suggests that each is important to the function of adult muscle. The similarity of time course may indicate that there is coordinate developmental regulation of slow calcium channels, charge movement, and the t-system.

DISCUSSION

During the first few weeks of postnatal development of the rat FDB muscle, the magnitude of the calcium current I_{slow}, the quantity of mobile charge measurable as voltage-dependent charge movement (Q_{max}), and the relative contribution of the t-system to linear fiber capacitance increase severalfold. A postnatal developmental increase is consistent with an important role for all three in the function of adult
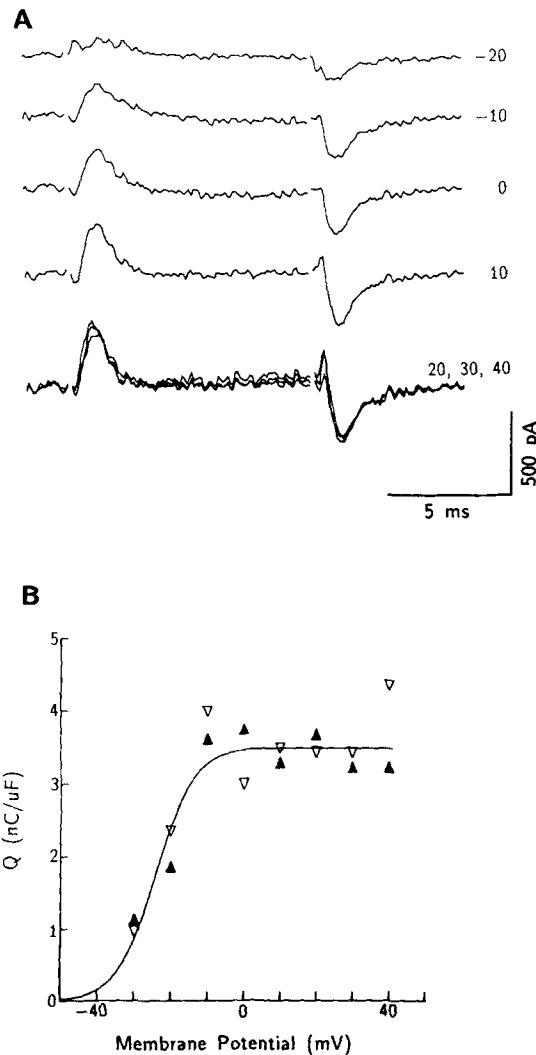
FIGURE 3. Slow, voltage-dependent charge movement is present in developing muscle fibers. The upper panels show charge movements from a 5-d (A) and a 21-d (C) FDB fiber; the charge movements were elicited by a 10-ms depolarization from the holding potential to the indicated test potentials. The lower panels illustrate, for the same two fibers, the dependence of Q_{ON} (filled triangles) and Q_{OFF} (open triangles) on the test potential. The smooth curves in B and D are plots of text Eq. 1 with values for Q_{max}, k, and $\bar{V}$ that were determined by a least-squares fitting procedure. (A and B) Fiber D29; 5-d FDB; whole-cell (single-electrode) patch clamp; 10 Ca solution with 1 mM $CdCl_2$ and 10 μM TTX; HP = −80; C = 135 pF. The control current was a 20-mV depolarization from the holding potential. At each test potential, the illustrated trace is the average of four separate test currents. For this fiber, Q_{max} = 3.5 nC/μF, k = 5.2 mV, and $\bar{V}$ = −24 mV. (C and D) (opposite) Fiber D81; 21-d FDB; two-electrode voltage clamp; 10 Ca solution + 10 μM TTX; HP = −80; C = 875 pF. The control pulse was a 30-mV depolarization; the traces illustrated are individual test currents without signal averaging. For this fiber, Q_{max} = 11.3 nC/μF, k = 12.2 mV, and $\bar{V}$ = −6 mV.

C

D
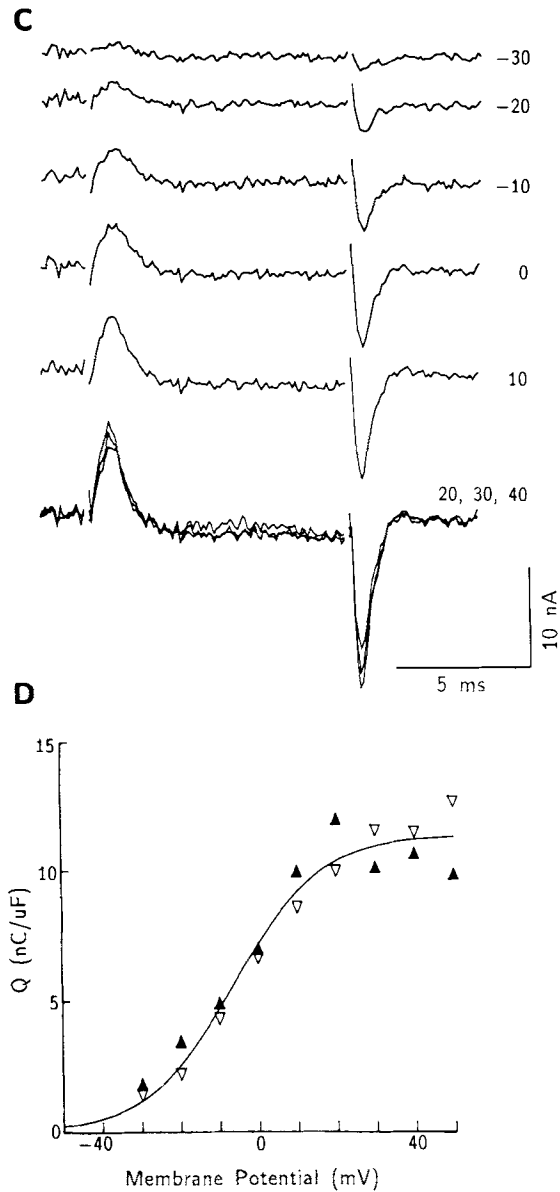
muscle cells. By contrast, the disappearance of the calcium current I_{fast} during post-natal development is obviously inconsistent with a role for this current in adult muscle.

Function of I_{fast}

One possible function for I_{fast}, to couple membrane excitation to contraction in developing muscle, is not supported by the available data. Thus, blocking I_{fast} (and also I_{slow}) does not prevent membrane depolarization from causing contraction of rat or mouse
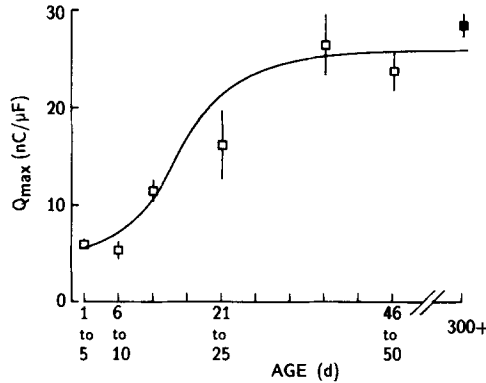
FIGURE 4.   Postnatal developmental increase in Q_{max}. Each data point represents the average value obtained for fibers spanning a 5-d range of age. Charge movements were measured as described in the Methods. Q_{max} was determined as the area under the ON transient for a test pulse to +40 mV. For each fiber, the value of Q_{max} was normalized by the linear fiber capacitance. The filled square is the value determined by Simon and Beam (1985a) from three-microelectrode measurements on adult rat omohyoid muscle fibers. Error bars indicate ± SEM. The smooth curve is the same one as in Fig. 2 B.

myotubes or neonatal rat FDB fibers (Knudson et al., 1986). Similarly, blocking calcium currents does not abolish E-C coupling in embryonic amphibian skeletal muscle (Huang, 1986). Because I_{fast} is seen in acutely dissociated fibers only during the first 2–3 wk postnatal, it is tempting to speculate that it plays a role in developmental events occurring during this period. One such event is myogenesis; in the rat lumbrical muscle, the number of fibers doubles during the first 2 wk postnatal (Betz et al., 1979). Perhaps I_{fast} plays a role in the fusion of myoblasts to form myotubes. Another significant developmental event that occurs during the first 2–3 wk postnatal is the shift from polyneuronal motor innervation to single-neuronal innervation of muscle fibers (Betz, 1987). Thus, one might imagine that I_{fast} somehow guides the elimination of supernumerary synapses. Alternatively, the presence or absence of I_{fast} may be under neural control such that maturation of the motor innervation causes the elimination of I_{fast}, as has been demonstrated for the apamin-sensitive Ca^{++}-activated K^+ channel in mammalian skeletal muscle (Schmid-Antomarchi et al., 1985). Establishing the developmental factors that cause the disappearance of I_{fast} should provide insights into the function of this current.
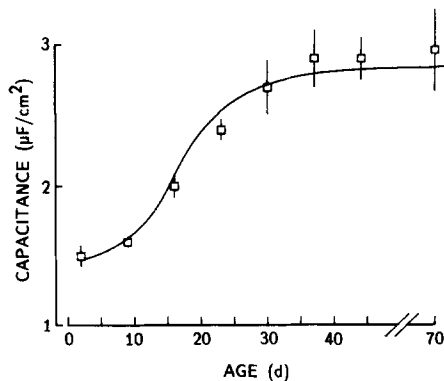

FIGURE 5.   Postnatal developmental increase in capacitance normalized by fiber surface area. For each fiber, the linear capacitance was measured as described in the Methods. Fiber surface area was calculated, under the assumption of right-cylindrical geometry, from visual measurements of fiber diameter and length. Error bars indicate ± SEM. The smooth curve is the same one as in Figs. 2 B and 4.

Developmental Shift in the Voltage Dependence of Charge Movement and I_{slow}

The steady state charge-voltage distribution for developing fibers was characterized in terms of the parameters k and $\bar{V}$, which appear in Eq. 1. The values of k determined in developing FDB fibers are similar to those determined for adult mammalian fast-twitch muscles (Hollingworth and Marshall, 1981; Dulhunty and Gage, 1983; Simon and Beam, 1985a; Lamb, 1986a). The value of $\bar{V}$ determined for FDB fibers from the oldest animals (>25 d) is ~15–20 mV more positive than the values for $\bar{V}$ determined for adult mammalian muscle (comparison of values for $\bar{V}$ requires taking into account differences in measurement conditions; see Discussion in Simon and Beam, 1985a). Independent of the absolute values for $\bar{V}$, our data suggest that there may be a developmental change in the steady state charge-voltage relationship. Thus, in FDB fibers from newborn animals, $\bar{V}$ was ~12 mV hyperpolarized compared with $\bar{V}$ for older animals. Denervation of adult mammalian fast-twitch muscle has been reported to produce a hyperpolarizing shift in $\bar{V}$ of about the same magnitude (Hollingworth et al., 1984; Dulhunty and Gage, 1985). During postnatal development, the voltage dependence for activation of I_{slow} shifted in the same direction as steady state charge distribution, although the shift for I_{slow} (~6 mV) was smaller.

Comparison of the Voltage Dependence of Charge Movement and I_{slow}

At least a portion of charge movement in skeletal muscle is necessarily involved in the gating of the slow calcium current, making it of interest to compare the voltage dependence of these two processes. At any given age, the average parameters determined by Boltzmann fits indicate that the dependence of the slow calcium conductance on potential is steeper and is centered at a more positive potential than steady state charge distribution. Thus, for the slow calcium conductance, the value of $\bar{V}$ is 12–20 mV depolarized, and the value of k (which is inversely related to steepness) is about half, relative to these parameters for steady state charge distribution. Interestingly, in single frog skeletal muscle fibers, the voltage dependence of the peak rate of SR calcium release is steeper and shifted positively compared to the voltage dependence of steady state charge distribution (Melzer et al., 1986), and these differences are similar in magnitude to those found by us for slow calcium conductance relative to charge movement. Thus, it appears that the voltage dependence of SR calcium release is similar to that for activation of slow calcium conductance. Although a direct comparison of these two processes has not been reported, Brum et al. (1987) have compared calcium current amplitudes with changes in myoplasmic calcium concentrations in single frog muscle fibers. Their results are consistent with a similar voltage dependence for activation of slow calcium conductance and peak SR calcium release.

Given a similar voltage dependence for activation of slow calcium conductance and SR calcium release, it seems a reasonable hypothesis that the same process (e.g., charge movement) controls both (Rios et al., 1986; Beam et al., 1986; Lamb and Walsh, 1987). Melzer et al. (1986) have described simple physical models in which charge movement accounts for the observed voltage dependence of SR calcium release. The same models would also be able to account for the voltage dependence of I_{slow} activation, although they would not explain why I_{slow} reaches its peak at a time

long after the movement of charge is essentially complete. For this, it seems necessary to postulate that after the movement of charge, at least one slow and relatively voltage-independent transition must occur before the slow calcium channel opens.

Tubular Origin of I_{slow} and Charge Movement

Studies of adult skeletal muscle imply that both I_{slow} and charge movement arise mainly, if not entirely, within the t-system. In frog skeletal muscle, the slow calcium channel current is eliminated by glycerol shock (Nicola Siri et al., 1980; Potreau and Raymond, 1980), a treatment that uncouples the t-system from the surface of the fiber. Also in frog skeletal muscle, studies of cut fibers demonstrate that the time-dependent decay of the slow calcium current during a prolonged depolarization is due to depletion of calcium from a restricted extracellular space having properties consistent with the t-system (Almers et al., 1981). In this regard, it is interesting that I_{slow} recorded from FDB fibers of older rats showed a more prominent decay during prolonged depolarization than I_{slow} from FDB fibers of younger rats (cf. Fig. 1). Because the fibers of older animals have a larger diameter and more extensive t-system, one would expect more significant calcium depletion than in fibers of younger animals (to be replenished, calcium must diffuse into the t-system from the fiber surface). In rat skeletal muscle, the effects of temperature on the charge movement time course (Simon and Beam, 1985a) and mathematical modeling of charge movement kinetics (Simon and Beam, 1985b) both indicate that the mobile charge is in the t-system. Experimental manipulations that alter the electrical coupling of the t-system to the fiber surface also imply a tubular location for the mobile charge in both frog (Campbell, 1986) and rabbit (Lamb, 1986a) skeletal muscle.

Does T-Tubular Growth Account for the Increases in I_{slow} and Q_{max}?

When normalized by total linear capacitance, peak I_{slow} and Q_{max} both increase postnatally. However, early in development, the t-system contributes a smaller proportion of the total linear capacitance than later in development (Fig. 5). Thus, the question arises: do Q_{max} and peak I_{slow} simply scale with the membrane area of the t-system? Our data do not permit us to answer this question. If the surface membrane is assumed to have a capacitance of 1 $\mu F/cm^2$, then the fraction of total capacitance contributed by the t-system approximately doubled during postnatal development (i.e., from 0.5/1.5 to 2.0/3.0). This doubling is much smaller than the approximately fivefold increase in normalized Q_{max} and I_{slow}. However, if the surface membrane is assumed to have a capacitance of 1.35 $\mu F/cm^2$, then the fractional contribution of the t-system to the total capacitance increased slightly more than fivefold postnatally (i.e., from 0.15/1.5 to 1.65/3.0), an increase sufficient to account for the increases in I_{slow} and Q_{max}. In frog skeletal muscle fibers, where it has been most extensively investigated, the capacitance referred to the right-cylindrical area of smooth fiber surface exceeds 1 $\mu F/cm^2$, with different workers having determined values ranging from 1.1 to >2.0 $\mu F/cm^2$ (Chandler and Schneider, 1976; Mathias et al., 1977; Takashima, 1985). The capacitance values exceeding 1.0 $\mu F/cm^2$ appear to be accounted for by folding and indentation of the fiber surface (Dulhunty and Franzini-Armstrong, 1975). Unfortunately, there are no data as to whether the folding and indentation of

the surface membrane of neonatal FDB fibers are sufficient to increase the surface capacitance to 1.35 $\mu F/cm^2$ and whether these geometric factors remain constant during development. Moreover, the subcellular distribution (tubular vs. surface) of charge movement and slow calcium channels may change postnatally. Thus, although Q_{max} and I_{slow} both increase faster than the total linear capacitance, it is uncertain whether Q_{max} and I_{slow} normalized only by t-system area remain constant or increase during postnatal development. However, even if Q_{max} and I_{slow} increase only as fast as the t-system, it still implies that both are important to adult muscle.

I_{slow}, Charge Movement, and Dihydropyridine Receptors

Kazazoglou et al. (1983) have determined that the number of dihydropyridine-binding sites (per milligram of protein) in rat leg skeletal muscle increases ~4.5-fold during the first 21 d postnatal. Both the time course and the magnitude of this increase are very similar to the time course and magnitude of the postnatal increases in I_{slow}, Q_{max}, and the t-system. Furthermore, dihydropyridine-binding sites appear to be localized preferentially in the t-system (Fosset et al., 1983; Glossman et al., 1983), just as are the channels responsible for I_{slow} and the mobile charge giving rise to charge movement (see above). These parallels are consistent with the growing body of evidence that, although calcium entry mediated by I_{slow} is not involved in E-C coupling, the slow calcium channel protein, or a closely related protein, is essential for E-C coupling. Thus, under appropriate conditions, the organic calcium channel antagonist D-600 causes paralysis of frog skeletal muscle (Eisenberg et al., 1983). Under these same conditions, D-600 abolishes charge movements (Hui et al., 1984). Similarly, nifedipine reduces both the magnitude of charge movement (Lamb, 1986b; Rios and Brum, 1987) and the transient of calcium release from the SR (Rios and Brum, 1987); both these effects are potentiated at depolarized holding potentials (Rios and Brum, 1987), as is the dihydropyridine block of calcium current (Bean, 1984; Cognard et al., 1986b; Beam and Knudson, 1988). Further evidence linking I_{slow}, charge movement, and dihydropyridine receptors is provided by studies of mice with muscular dysgenesis, a recessive mutation that causes E-C coupling in skeletal muscle to fail (Powell and Fambrough, 1973; Klaus et al., 1983). Dysgenic skeletal muscle cells lack I_{slow} (Beam et al., 1986) and have only about one-fifth as many dihydropyridine receptors as normal muscle (Pincon-Raymond et al., 1985).

During E-C coupling, calcium is released from the SR in response to a change in potential across the t-system membrane. Thus, there must be "sensor" molecules in the t-tubular membrane whose state alters when potential across the t-system changes. Schneider and Chandler (1973) suggested that these hypothetical sensor molecules are responsible for the signal measured as charge movement. Recently, Rios and Brum (1987) have proposed that the molecule that generates charge movement is the skeletal muscle dihydropyridine receptor. Since dihydropyridines block I_{slow}, one would expect that the slow calcium channel is also a dihydropyridine receptor. Perhaps the same molecule that generates charge movement also gives rise to I_{slow} (Rios et al., 1986; Beam et al., 1986; Lamb and Walsh, 1987). Specifically, one might imagine that the charge movement molecule represents a modified calcium channel protein whose main function is to sense t-system potential and control SR calcium

release, but which also maintains the function of gating calcium entry across the t-tubular membrane, even though this calcium movement is not directly involved in E-C coupling. Alternatively, the molecule that generates charge movement and the one that gives rise to I_{slow} may represent closely related proteins, both of which are affected by dihydropyridines in a voltage-dependent manner. In either case, the function, if any, of I_{slow} itself remains unidentified.

REFERENCES

Adrian, R. H., and W. Almers. 1976. Charge movement in the membrane of striated muscle. *Journal of Physiology.* 254:339–360.

Almers, W., R. Fink, and P. T. Palade. 1981. Calcium depletion in frog muscle tubules: the decline of calcium current under maintained depolarization. *Journal of Physiology.* 312:177–207.

Almers, W., and P. T. Palade. 1981. Slow calcium and potassium currents across frog muscle membrane: measurements with a vaseline-gap technique. *Journal of Physiology.* 312:159–176.

Beam, K. G., and C. M. Knudson. 1988. Calcium currents in embryonic and neonatal mammalian skeletal muscle. *Journal of General Physiology.* 91:781–798.

Beam, K. G., C. M. Knudson, and J. A. Powell. 1986. A lethal mutation in mice eliminates the slow calcium current in skeletal muscle cells. *Nature.* 320:168–170.

Bean, B. P. 1984. Nitrendipine block of cardiac calcium channels: high-affinity binding to the inactivated state. *Proceedings of the National Academy of Sciences.* 81:6388–6392.

Beaty, G. N., and E. Stefani. 1976. Inward calcium current in twitch muscle fibers of the frog. *Journal of Physiology.* 260:27P. (Abstr.)

Betz, W. J. 1987. Motoneuron death and synapse elimination in vertebrates. *In* The Vertebrate Neuromuscular Junction. Alan R. Liss, Inc., New York, NY. 117–162.

Betz, W. J., J. H. Caldwell, and R. R. Ribchester. 1979. The size of motor units during postnatal development of rat lumbrical muscle. *Journal of Physiology.* 279:463–478.

Brum, G., E. Stefani, and E. Rios. 1987. Ca^{++} currents and intracellular Ca^{++} concentrations in single skeletal muscle fibers of the frog. *Biophysical Journal.* 51:198a. (Abstr.)

Campbell, D. T. 1986. Charge movements measured during transverse-tubular uncoupling in frog skeletal muscle. *Biophysical Journal.* 50:329–338.

Carlsen, R. C., D. B. Larson, and D. A. Walsh. 1985. A fast-twitch oxidative-glycolytic muscle with a robust inward calcium current. *Canadian Journal of Physiology and Pharmacology.* 63:958–965.

Chandler, W. K., R. F. Rakowski, and M. F. Schneider. 1976. A non-linear voltage dependent charge movement in frog skeletal muscle. *Journal of Physiology.* 254:245–283.

Chandler, W. K., and M. F. Schneider. 1976. Time course of potential spread along a skeletal muscle fiber under voltage clamp. *Journal of General Physiology.* 67:165–184.

Cognard, C., M. Lazdunski, and G. Romey. 1986a. Different types of Ca^{2+} channels in mammalian skeletal muscle cells in culture. *Proceedings of the National Academy of Sciences.* 83:517–521.

Cognard, C., G. Romey, J.-P. Galizzi, M. Fosset, and M. Lazdunski. 1986b. Dihydropyridine-sensitive Ca^{2+} channels in mammalian skeletal muscle cells in culture: electrophysiological properties and

interactions with Ca^{2+} channel activator (Bay K8644) and inhibitor (PN 200-110). *Proceedings of the National Academy of Sciences.* 83:1518–1522.

Costantin, L. L. 1975. Contractile activation in skeletal muscle. *Progress in Biophysics and Molecular Biology.* 29:197–224.

Donaldson, P. L., and K. G. Beam. 1983. Calcium currents in a fast-twitch skeletal muscle of the rat. *Journal of General Physiology.* 82:449–468.

Dulhunty, A. F., and C. Franzini-Armstrong. 1975. The relative contribution of the folds and caveolae to the surface membrane of frog skeletal muscle fibers at different sarcomere lengths. *Journal of Physiology.* 250:513–539.

Dulhunty, A. F., and P. W. Gage. 1983. Asymmetrical charge movement in slow- and fast-twitch mammalian muscle fibers in normal and paraplegic rats. *Journal of Physiology.* 341:213–231.

Dulhunty, A. F., and P. W. Gage. 1985. Excitation-contraction coupling and charge movement in denervated rat extensor digitorum longus and soleus muscles. *Journal of Physiology.* 358:75–89.

Eisenberg, R. S., R. T. McCarthy, and R. L. Milton. 1983. Paralysis of frog skeletal muscle fibers by the calcium antagonist D-600. *Journal of Physiology.* 341:495–505.

Endo, M. 1977. Calcium release from the sarcoplasmic reticulum. *Physiological Reviews.* 57:71–108.

Endo, M., M. Tanaka, and Y. Ogawa. 1970. Calcium induced release of calcium from the sarcoplasmic reticulum in skinned muscle fibers. *Nature.* 228:34–36.

Ford, L. E., and R. J. Podolsky. 1970. Regenerative calcium release within muscle cells. *Science.* 167:58–59.

Fosset, M., E. Jaimovitch, E. Delpont, and M. Lazdunski. 1983. [^{3}H]Nitrendipine receptors in skeletal muscle. Properties and preferential localization in transverse tubules. *Journal of Biological Chemistry.* 258:6086–6092.

Glossmann, H., D. R. Ferry, and C. B. Boschek. 1983. Purification of the putative calcium channel from skeletal muscle with the aid of [^{3}H]-nimodipine binding. *Naunyn-Schmiedeberg's Archives of Pharmacology.* 323:1–11.

Gonzalez-Serratos, H., R. Valle-Aguilera, D. A. Lathrop, and M. del Carmen Garcia. 1982. Slow inward currents have no obvious role in excitation-contraction coupling. *Nature.* 298:292–294.

Hamill, O. P., A. Marty, E. Neher, B. Sakmann, and F. J. Sigworth. 1981. Improved patch-clamp techniques for high-resolution current recording from cells and cell-free membrane patches. *Pflügers Archiv.* 391:85–100.

Hollingworth, S., and M. W. Marshall. 1981. A comparative study of charge movement in rat and frog skeletal muscle fibers. *Journal of Physiology.* 321:583–602.

Hollingworth, S., M. W. Marshall, and E. Robson. 1984. Ionic currents and charge movements in organ-cultured rat skeletal muscle. *Journal of Physiology.* 357:369–386.

Horowicz, P., and M. F. Schneider. 1981. Membrane charge movement in contracting and noncontracting skeletal muscle fibers. *Journal of Physiology.* 314:565–593.

Huang, C. L.-H. 1986. Contractile activation of myotomes from developing larvae of *Xenopus laevis*. *Journal of Physiology.* 375:391–401.

Hui, C. S., R. L. Milton, and R. S. Eisenberg. 1984. Charge movement in skeletal muscle fibers paralyzed by the calcium-entry blocker D600. *Proceedings of the National Academy of Sciences.* 81:2582–2585.

Kazazoglou, T., A. Schmid, J.-F. Renaud, and M. Lazdunski. 1983. Ontogenic appearance of Ca^{2+} channels characterized as binding sites for nitrendipine during development of nervous, skeletal and cardiac muscle systems in the rat. *FEBS Letters.* 164:75–79.

Klaus, M. M., P. S. Stylianos, J. M. Rapalus, R. T. Briggs, and J. A. Powell. 1983. Evidence for

dysfunction in the regulation of cytosolic Ca^{2+} in excitation-contraction uncoupled dysgenic muscle. *Developmental Biology.* 99:152–165.

Knudson, C. M., S. D. Jay, and K. G. Beam. 1986. Developmental increase in skeletal muscle slow calcium current. *Biophysical Journal.* 49:13a. (Abstr.)

Lamb, G. D. 1986a. Asymmetric charge movement in contracting muscle fibers in the rabbit. *Journal of Physiology.* 376:63–83.

Lamb, G. D. 1986b. Components of charge movement in rabbit skeletal muscle: the effect of tetracaine and nifedipine. *Journal of Physiology.* 376:85–100.

Lamb, G. D., and T. Walsh. 1987. Calcium currents, charge movement and dihydropyridine binding in fast- and slow-twitch muscles of rat and rabbit. *Journal of Physiology.* 393:595–617.

Luff, A. R., and H. L. Atwood. 1971. Changes in the sarcoplasmic reticulum and transverse tubular system of fast and slow skeletal muscles of the mouse during postnatal development. *Journal of Cell Biology.* 51:369–383.

Mathias, R. T., R. S. Eisenberg, and R. Valdiosera. 1977. Electrical properties of frog skeletal muscle fibers interpreted with a mesh model of the tubular system. *Biophysical Journal.* 17:57–93.

Melzer, W., M. F. Schneider, B. J. Simon, and G. Szucs. 1986. Intramembrane charge movement and calcium release in frog skeletal muscle. *Journal of Physiology.* 373:481–511.

Nicola Siri, L., J. A. Sanchez, and E. Stefani. 1980. Effect of glycerol treatment on the calcium current of frog skeletal muscle. *Journal of Physiology.* 305:87–96.

Pincon-Raymond, M., F. Rieger, M. Fosset, and M. Lazdunski. 1985. Abnormal transverse tubule system and abnormal amount of receptors for Ca^{2+} channel inhibitors of the dihydropyridine family in skeletal muscle from mice with embryonic muscular dysgenesis. *Developmental Biology.* 112:458–466.

Potreau, D., and G. Raymond. 1980. Slow inward barium current and contraction on frog single muscle fibers. *Journal of Physiology.* 303:91–109.

Powell, J. A., and D. M. Fambrough. 1973. Electrical properties of normal and dysgenic mouse skeletal muscle in culture. *Journal of Cellular Physiology.* 82:21–38.

Rios, E., and G. Brum. 1987. Involvement of dihydropyridine receptors in excitation-contraction coupling in skeletal muscle. *Nature.* 325:717–720.

Rios, E., G. Brum, and E. Stefani. 1986. E-C coupling effects of interventions that reduce slow Ca current suggest a role of t-tubule Ca channels in skeletal muscle function. *Biophysical Journal.* 49:13a. (Abstr.)

Sanchez, J. A., and E. Stefani. 1978. Inward calcium current in twitch muscle fibers of the frog. *Journal of Physiology.* 283:197–209.

Schiaffino, S., and A. Margreth. 1969. Coordinated development of the sarcoplasmic reticulum and T system during postnatal differentiation of rat skeletal muscle. *Journal of Cell Biology.* 41:855–875.

Schmid-Antomarchi, H., J.-F. Renaud, G. Romey, M. Hugues, A. Schmid, and M. Lazdunski. 1985. The all-or-none role of innervation in expression of apamin receptor and of apamin-sensitive Ca^{2+}-activated K^+ channel in mammalian skeletal muscle. *Proceedings of the National Academy of Sciences.* 82:2188–2191.

Schneider, M. F., and W. K. Chandler. 1973. Voltage dependent charge movement in skeletal muscle: a possible step in excitation-contraction coupling. *Nature.* 242:244–246.

Simon, B. J., and K. G. Beam. 1983. Charge movement in a fast twitch skeletal muscle from rat. *Biophysical Journal.* 41:223–226.

Simon, B. J., and K. G. Beam. 1985a. Slow charge movement in mammalian skeletal muscle. *Journal of General Physiology.* 85:1–19.

Simon, B. J., and K. G. Beam. 1985*b*. The influence of transverse tubular delays on the kinetics of charge movement in mammalian skeletal muscle. *Journal of General Physiology.* 85:21–42.

Stanfield, P. R. 1977. A calcium-dependent inward current in frog skeletal muscle fibers. *Pflügers Archiv.* 368:267–270.

Takashima, S. 1985. Passive electrical properties and voltage dependent membrane capacitance of single skeletal muscle fibers. *Pflügers Archiv.* 403:197–204.

Walsh, K. B., S. H. Bryant, and A. Schwartz. 1986. Effect of calcium antagonist drugs on calcium currents in mammalian skeletal muscle fibers. *Journal of Pharmacology and Experimental Therapeutics.* 236:403–407.